Excitation functions and isomeric cross section ratio of the $^{58}Ni(n,p)^{58}Co^{m,g}$ reactions from 2 to 15 MeV

Cs. M. Buczkó,[1,*] J. Csikai,[1] S. Sudár,[1] Á. Grallert,[1] S. A. Jonah,[2] B. W. Jimba,[2] T. Chimoye,[3] and M. Wagner[4]
[1]*Institute of Experimental Physics, Kossuth University, 4001 Debrecen, Postfach 105, Hungary*
[2]*Centre for Energy Research and Training, Ahmadu Bello University, Zaria, Nigeria*
[3]*Faculty of Science and Technology, Thammassat University, Bangkok, Thailand*
[4]*Institut für Radiumforschung und Kernphysik, der Universität Wien, A-1090 Wien, Boltzmangasse 3, Austria*
(Received 10 January 1995)

The cross sections for the $^{58}Ni(n,p)^{58}Co^{m,g}$ reactions were measured in the neutron energy range 2.1–14.8 MeV using the activation technique in combination with high-resolution gamma-ray spectroscopy. Neutrons were produced via the $^{2}H(d,n)^{3}He$ and $^{3}H(d,n)^{4}He$ reactions using solid TiD, TiT, and deuterium gas targets. The isomeric cross section ratio was determined in the 5.38–12.2 MeV range and at 14.8 MeV neutron energy. Statistical model calculations taking into account precompound effects were performed for the formation of the isomeric and ground states of the ^{58}Co. The calculational results based on the "back-shifted" level density model agree well with the measured excitation functions and render possible the selection of the most probable values of isomeric cross section ratios among the discrepant data obtained around 2 and 14 MeV neutron energies.

PACS number(s): 24.60.Dr, 25.40.−h, 28.20.−v

I. INTRODUCTION

Precise knowledge of the excitation functions of $^{58}Ni(n,p)^{58}Co^{m,g}$ reactions from the threshold to about 20 MeV are of considerable importance for testing nuclear reaction models and for various applications, especially in fast-neutron dosimetry and spectral measurements related to the fusion reactor technology as well as in radiation damage studies. Investigation of the energy dependence of the isomeric cross section ratio gives information on the role of spin values in the formation of isomeric states. The cross section curves, $\sigma_{act}=\sigma^m+\sigma^g$, of the $^{58}Ni(n,p)^{58}Co$ reaction measured by a number of investigators (cf. Refs. [1–8]) show a large spread, especially in the 8–12 MeV range, therefore, the evaluated (cf. Refs [9,10]) data are also discrepant. The model calculations (cf. Refs. [11,12]) for the $\sigma^g(E)$ and $\sigma^m(E)$ functions based on different parameters are inconsistent. A survey of the available literature (cf. Refs. [13–16]) indicates that the isomeric cross section ratio has not been measured in the energy range between 5 and 13 MeV because of the unfavorable decay scheme of $^{58}Co^m$ and the difficulties in the determination of the flux density spectra of incident neutrons. Since nickel is an important structural material in fission and fusion reactor technologies, the measured data could give useful information on hydrogen-gas production as a function of neutron energy. In this work experimental and theoretical studies were performed on the $^{58}Ni(n,p)^{58}Co^{m,g}$ reactions in the neutron energy range 2–15 MeV.

II. EXPERIMENTAL PROCEDURE

High purity (Goodfellow) natural nickel foils of 19 mm diam and 1 mm thick were irradiated with neutrons for 4–10 h depending on the flux density values at different energies. Energy and fluence monitor foils (summarized in Table I) of the same size as the sample were attached in front and at the back of each sample. Irradiations with 2.1–2.9 MeV and 13.5–14.8 MeV neutrons were carried out at the neutron generator of the Institute of Experimental Physics, Kossuth University, Debrecen, in a low scattering arrangement (cf. Ref. [17]). Neutrons were produced via the $^{2}H(d,n)^{3}He$ and $^{3}H(d,n)^{4}He$ reactions using (220±5) keV and (180±5) keV magnetically analyzed deuteron beams, respectively. Thick solid TiD and TiT targets cooled with liquid N_2 and air jet were used for the relative measurement of the cross section curve. For normalization, the absolute values of the cross sections at 2.9 MeV and 14.1 MeV have been determined with thin TiD and TiT targets, respectively. The foil stacks were placed at different angles relative to the deuteron beam direction to change the average neutron energies within the samples. Neutrons in the energy range of 5.38–12.38 MeV were produced by the variable energy cyclotron MGC-20 of ATOMKI, Debrecen, using a D_2 gas target. The gas cell of 4 cm long and 4 cm diam filled up to 1.8×10^5 Pa pressure has been closed with Mo or Nb entrance foils and W beam stop (cf. Ref. [18]). The thicknesses of the Mo, Nb, and W foils were 8, 5, and 200 μm, respectively. The Mo window was replaced by a thin Nb foil in the second series of irradiations at 8.92, 9.6, 11.13, and 12.20 MeV neutron energies. The samples were placed in the 0° direction relative to the deuteron beam, at different distances between 2 and 4 cm from the back of the beam stop. The average beam current was about 3 μA. The variation of the neutron flux density in time has been recorded by a "long-counter" containing a BF_3 detector with the necessary electronics.

The absolute activity of the irradiated foils was determined by using a HPGe detector. The peak area analysis was based on the program ACCUSPEC developed for IBM compatible personal computers. The relative activity of the Ni foils

*Author to whom correspondence should be addressed.

TABLE I. Reactions and nuclear data used in the measurements.

Neutron energy (MeV)	Fluence and energy monitor reactions	$T_{1/2}$	E_γ (keV)	I_γ (%)
2.1–2.9	$^{238}U(n,f)$			
	$^{115}In(n,n')^{115m}In$	4.49 h	336	45.91
5.38–12.38	$^{115}In(n,n')^{115m}In$	4.49 h	336	45.91
	$^{27}Al(n,\alpha)^{24}Na$	15.03 h	1368	100
	$^{27}Al(n,p)^{24}Na$	9.46 m	844	73.1
	$^{56}Fe(n,p)^{56}Mn$	2.579 h	847	98.87
	$^{90}Zr(n,2n)^{89}Zr$	78.44 h	909	99.01
	$^{48}Ti(n,p)^{48}Sc$	43.7 h	983.5	100
			1037.7	97.5
			1312.1	100
	$^{59}Co(n,\alpha)^{56}Mn$	2.58 h	846.8	98.87
	$^{58}Ni(n,p)^{58}Co^{g,m}$	70.78 d	810.76	99.44
	$^{197}Au(n,2n)^{196}Au$	6.18 d	355.7	87
	$^{238}U(n,f)$			
13.52–14.48	$^{93}Nb(n,2n)^{92m}Nb$	10.15 d	934	100
	$^{27}Al(n,\alpha)^{24}Na$	15.03 h	1368	100

as a function of time was measured by a NaI(Tl) detector. The absolute efficiency curves both for the HPGe and NaI(Tl) detectors have been determined by standard sources (cf. Refs. [19,20]).

The sample counts were corrected for the following effects; variation of the flux in time, gamma-ray self-absorption, true coincidence, dead-time, irradiation, and measuring geometries, neutron attenuation in the sample. The errors of the cross sections given in Tables II–IV contain also the following principal sources: counting statistics, detector efficiency, sample masses, decay constants, energy and fluence uncertainties, and reference cross sections.

In addition to the foil activation method, the neutron flux density has also been determined at $E_n=(2.87\pm0.04)$ MeV by a fission chamber using a thin (0.2 mg/cm^2) depleted ^{238}U layer and a special measuring technique (cf. Ref. [21]). The $\sigma_{act}=\sigma^m+\sigma^g$ data for the $^{58}Ni(n,p)^{58}Co$ reaction were determined relative to the $^{238}U(n,f)$ monitor cross section. The induced activity of the Ni foil was measured with high precision after the complete decay of $^{58}Co^m$ using a well-type NaI(Tl) detector of about 1600 cm^3. Integral γ-ray counting was performed above the energy discrimination level of 22.1 keV. The effective neutron energy profile and the average energy of the neutrons incident on the Ni sample and U layer were calculated by means of the Monte Carlo simulation code PROFILE (cf. Ref. [22]) adapted to the $^2H(d,n)^3He$ reaction, taking into account the slowing down and the energy-dependent scattering of the deuterium ions in the target. The decay data accepted in this work for the determination of the $^{58}Ni(n,p)^{58}Co^{m,g}$ reaction cross sections are summarized in Table I (cf. Ref. [23]).

Considering the fact that there are two energy groups of neutrons produced in the $^2H(d,n)^3He$ reaction at $E_d\geq5$ MeV even in the net spectral yield (cf. Ref. [24]), the flux density spectra have been determined by the activation unfolding method at different incident deuteron energies. As can be seen in Fig. 1, breakup neutrons produced in both the Coulomb field and the $^2H(d,np)$ reaction are present in the spectrum with a high yield at $E_d=8$ MeV. These neutrons can contribute significantly to the ^{58}Co activity because of the low threshold of the $^{58}Ni(n,p)$ reaction. The same holds for the fluence monitor reactions. In the knowledge of the energy dependence of the reaction rate $[\phi(E)\sigma(E)]$, this contribution can be taken into account. The $\phi(E)$ values were determined by the activation unfolding method, while for $\sigma(E)$ the evaluated data from Ref. [9] based on the previous measurements have been accepted. For the determination of the cross section for the $^2H(d,n)$ monoenergetic neutrons, the reaction rate integrated over the group of low energy neutrons was subtracted from the total value obtained by experiment. The magnitude of the correction for the lower energy neutrons depends strongly on the bombarding deuteron energy for $E_d>7$ MeV. In the present experiment the correction was 1–35 % for the $E_d=3.16$–9.72 MeV interval, which corresponds to the $E_n=5.38$–12.38 MeV monoenergetic neutron range. The contribution of the low energy neutron group to the total activity of ^{58}Co produced in the $^{58}Ni(n,p)$ reaction does not exceed 4% in the $E_n=5.38$–9.6 MeV range. Therefore, a 30% uncertainty in the determination of the flux density spectra can cause about 1.5% error in the cross sections. Although the contribution of the low energy neutron group to the reaction rate increases significantly for $E_n>10$ MeV the error of the cross sections are almost the same because the determination of the $\Phi(E)$ function by unfolding method is more precise. The spectral shape of high energy neutrons measured by the pulse height response spectrometric (PHRS) system was used as input data for the activation unfolding. The main advantage of the activation unfolding or neutron spectrometric methods using an improved signal-to-background experimental arrangement (cf. Refs. [18,25]) is that only a single irradiation is required with gas in, and the effect of all low energy neutrons can be taken into account. In Fig. 1 the flux density spectra of neu-

TABLE II. Measured and calculated total (n,p) cross sections for ^{58}Ni.

Neutron energy (MeV)	Measured $\sigma(n,p)$ (mb)	Neutron energy (MeV)	Calculated $\sigma(n,p)$ (mb)
2.15±0.034	74±2.2	0.61	0.035
2.21±0.032	77±2.3	1.26	4.421
2.28±0.030	85±2.5	1.91	35.07
2.38±0.028	101±3.0	2.56	145.3
2.48±0.027	107±3.2	3.22	286.6
2.58±0.030	104±3.1	3.87	388.3
2.69±0.031	133±4.0	4.52	476.4
2.80±0.045	151±4.5	5.17	560.1
2.86±0.050	180±5.4	5.82	608.8
2.92±0.055	194±5.8	6.47	635.1
2.94±0.070	203±6.1	7.12	645.0
5.38±0.06	538±27	7.77	646.6
5.89±0.06	576±29	8.42	644.2
6.39±0.06	617±31	9.08	639.4
6.80±0.06	657±33	9.73	633.4
8.02±0.06	681±34	10.38	626.1
8.43±0.06	683±34	11.03	614.1
8.92±0.06	667±33	11.68	590.1
9.60±0.06	668±33	12.33	548.4
10.95±0.07	631±32	12.98	492.1
11.13±0.07	613±31	13.63	430.2
12.20±0.08	559±28	14.28	370.7
12.38±0.08	526±26	14.93	318.1
13.52±0.07	401±12	15.59	274.1
14.10±0.07	340±10	16.24	238.5
14.46±0.084	319±16		
14.74±0.135	288±14		
14.84±0.170	281±14		

TABLE III. Measured, deduced, and calculated isomeric cross section ratios for ^{58}Ni(n,p) reaction.

Neutron energy (MeV)	Measured (σ_m/σ_g)	Deduced (σ_m/σ_g)	Calculated (σ_m/σ_g)
5.38±0.06	0.54±0.01		0.56
5.89±0.06	0.55±0.01		0.57
6.39±0.06	0.52±0.01		0.59
6.80±0.06	0.61±0.02		0.60
8.02±0.06	0.62±0.02		0.64
8.43±0.06	0.62±0.02		0.65
8.67±0.06		0.65±0.05	0.66
8.92±0.06	0.64±0.02		0.67
9.13±0.06		0.69±0.05	0.68
9.59±0.06		0.79±0.06	0.69
9.60±0.06	0.79±0.02		0.70
10.04±0.07		0.66±0.05	0.71
11.13±0.07	0.77±0.02		0.74
12.20±0.08	0.71±0.02		0.77
14.84±0.17	1.08±0.03		0.81
16.24			0.83

TABLE IV. Deduced and calculated cross sections for the $^{58}Ni(n,p)^{58}Co^{m}$ reaction.

Neutron energy (MeV)	Deduced σ_m (mb)	Calculated σ_m (mb)	Neutron energy (MeV)	Deduced σ_m (mb)	Calculated σ_m (mb)
0.61		0.01	8.43±0.06	261±18	255.00
1.26		1.53	8.92±0.06	247±17	257.56
1.91		10.23	9.08		258.39
2.56		40.00	9.60±0.06	294±20	260.34
3.22		86.52	9.73		260.83
3.87		129.20	10.38		262.28
4.52		166.30	11.03		261.05
5.17		200.30	11.13±0.07	266±18	260.32
5.38±0.06	168±12	207.02	11.68		254.23
5.82		221.10	12.20±0.08	231±16	242.01
5.89±0.06	210±14	222.50	12.33		239.01
6.39±0.06	220±15	233.40	12.98		216.70
6.47		235.11	13.63		191.09
6.80±0.06	254±18	239.50	14.28		165.87
7.12		243.92	14.84±0.17	145±10	147.50
7.77		250.13	14.93		143.25
8.02±0.06	259±18	252.00	15.59		124.00
8.42		254.86	16.24		108.35

trons obtained by activation unfolding and pulse height response spectrometic (cf. Ref. [26]) methods are compared. The possible use of the unfolded pulse height distributions produced in an NE213 scintillator for the measurement of the neutron spectra above $E_n \geq 2$ MeV has been tested by the determination of the Maxwellian temperature T of ^{252}Cf neutrons. A value of $T = 1.418 \pm 0.01$ MeV was found in a good agreement with the recommended data, $T = 1.42$ MeV, obtained by other methods (cf. Ref. [27]). In addition, the spectrometer was calibrated by D-D and D-T neutrons using the associated particle method (APM) and also by a Pu-Be neutron source.

A systematic study of neutron spectra obtained by the foil activation and PHRS methods of $E_d < 10$ MeV has indicated that more precise excitation functions were required for the dosimetry reactions. In general, the activation method gives lower average energy and higher energy spread than the PHRS system. The main disadvantage of the unfolded pulse height distribution method is its high threshold ($E_n \geq 1.5$ MeV) which prevents the detection of the low energy neutrons, as shown in Fig. 1.

III. NUCLEAR MODEL CALCULATIONS

Cross section calculations in this work were done using the statistical model taking into account the preequilibrium effects. The calculational code STAPRE (cf. Ref. [28]) was used. Direct interactions were not considered but their contribution should be $< 10\%$. Neutron, proton, and alpha emission was taken into account and the transmission coefficients for these particles were calculated by the optical model code SCAT-2 (cf. Ref. [29]). The parameters for the optical model (OM) were chosen from a global parameter set. For neutron the OM parameter set of Becchetti and Greenlees (cf. Ref. [30]), while for proton those of Perey (cf. Ref. [31]) were used. In the case of alpha particles the OM parameters of McFadden and Satchler (cf. Ref. [32]) modified by Uhl *et al.* (cf. Ref. [33]) was used. For the energy and mass number dependence of the effective matrix element, $|M|^2 = (FM)A^{-3}E^{-1}$ formula was accepted with value of $FM = 500$. The separation energies of the emitted particles were taken from Ref. [34]. For the calculation of the isomeric cross section ratio the first 22 discrete levels of the ^{58}Co were used. The energies, spin, parities, and branching ratios of the discrete levels were selected from Ref. [35]. In the continuum region the level density was calculated by the "back-shifted" formula (cf. Ref. [36]) using the level density parameters given in Ref. [36]. In general, if these parameters were not available they could be estimated from the systematics and from the values of the neighboring isotopes. Occasionally, the level density parameters of **a** and Δ were varied

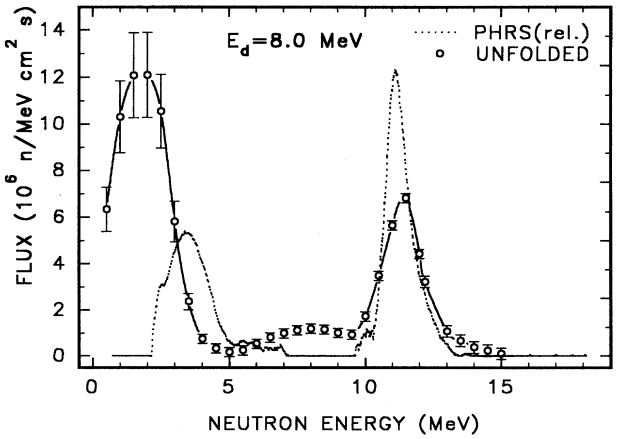

FIG. 1. A comparison of neutron spectra measured by activation unfolding and PHRS methods.

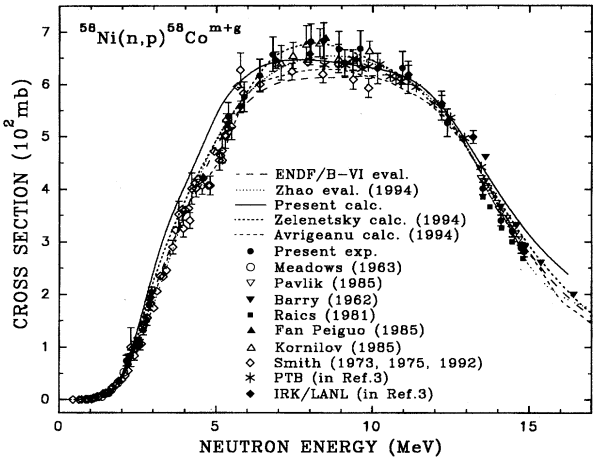

FIG. 2. A comparison of the measured, calculated, and evaluated excitation functions of the ^{58}Ni$(n,p)^{58}$Co^{m+g} reactions.

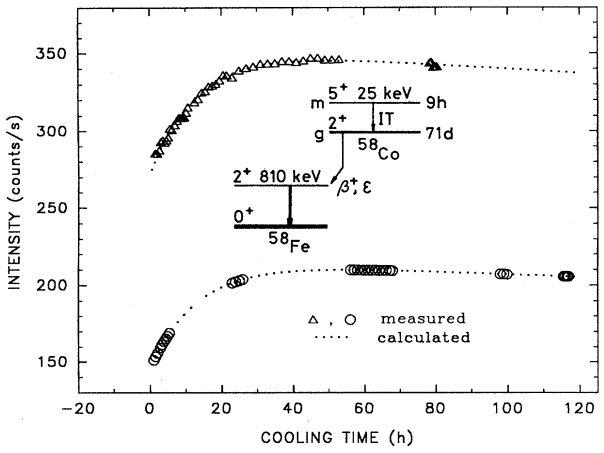

FIG. 3. Measured and calculated intensities vs cooling time in the decay of ^{58}Co^{m+g}.

within their uncertainties to check their effect on the cross sections. The spin distribution of the level density was characterized by the ratio of the effective moment of inertia Θ_{eff} to the rigid body, Θ_{rig}, value ($\eta=\Theta_{\text{eff}}/\Theta_{\text{rig}}$). The calculations were performed for $\eta=1.0$. The transmission coefficients of photons were calculated from the gamma-ray strength functions. For the $E1$ radiation the Brink-Axel model with global parameters, while for the $M1$, $E2$, $M2$, $E3$, and M3 radiation the Weisskopf model was used.

IV. RESULTS AND CONCLUSIONS

The measured activation cross sections for the formation of the isomeric and ground states of the ^{58}Co produced in the ^{58}Ni(n,p) reaction together with the calculated data are given in Table II. For a comparison the σ_{act} data measured and calculated in this investigation together with the literature values are presented in Fig. 2. As can be seen, the experimental results agree well with the Zelenetsky's calculation [11] in the whole energy range using the "super-fluid" level density model in the STAPRE code. Our calculations based on the "back-shifted" level density with $\eta=1.0$ give acceptable agreement with the measured data from the threshold to 15 MeV except in the 3–5 MeV range. This deviation may arise from the different optical potential used in the neutron channel. In Avrigeanu's calculation [12] the STAPRE-H code was used, which is an extension of the STAPRE program by the "geometry-dependent hybrid model" for the preequilibrium estimation. This model gives about 10–15 % lower values than the measured cross sections in the 5–10 MeV energy range, while in other regions describes well the experimental data. The evaluation of Zhao *et al.* (cf. Ref. [9]) deviate from the ENDF/B-VI (cf. Ref. [10]) recommendation especially at around 11 MeV, in agreement with our experimental data.

In addition to the total activation cross sections the isomeric cross section ratio has also been determined in the energy range 5.38–14.84 MeV. The decay scheme of the ^{58}Co shown in Fig. 3 renders possible the determination of the cross sections for the formation of both the isomeric and ground states via the detection of the same 810 keV gamma line emitted in the decay of ^{58}Co^{g}. The number of ground state atoms as a function of cooling time (t) is given by the following relation:

$$N_g(t)=\Phi n\left[\left(\frac{(\sigma_m\alpha+\sigma_g)}{\lambda_g}+\frac{\sigma_m\alpha}{\lambda_m-\lambda_g}\right)(1-e^{-\lambda_g t_{irr}})e^{-\lambda_g t}-\frac{\sigma_m\alpha}{\lambda_m-\lambda_g}(1-e^{-\lambda_m t_{irr}})e^{-\lambda_m t}\right], \quad (1)$$

where m and g refer to the metastable and ground state, N_g is the number of ground state atoms, t is the cooling time interval measured from the end of irradiation to the beginning of measurement, λ_g, λ_m, and σ^g, σ^m are the decay constants and the cross sections of ^{58}Co^{g} and ^{58}Co^{m}, respectively, Φ is the neutron flux density, n is the number of ^{58}Ni atoms in the sample, t_{irr} is the irradiation time, and α is the branching ratio in the decay of the ^{58}Co^{m} metastable state. The decay data adopted for the isomers of ^{58}Co (cf. Ref. [23]) were

^{58}Co^{m}: $T_{1/2}=9.15$ h, $E_\gamma=810.76$ keV,

I_{IT}(branching ratio)$=100\%$, $\alpha=1$,

^{58}Co^{g}: $T_{1/2}=70.78$ d, $E_\gamma=810.76$ keV, $I_\gamma=99.44\%$.

By measuring the peak areas of the 810 keV gamma line as a function of cooling time the σ^m/σ^g ratio could be deduced. The intensity values $I(t)$, obtained experimentally were approximated by the sum of two exponential functions using an appropriate computer code. Typical intensity-cooling time functions shown in Fig. 3 clearly indicate the good fit of Eq. (1) to the measured data. The relation between the measured intensity and the preexponential constants, A and B, containing the σ^m and σ^g values as unknown parameters is given by

$$I(t)=\Phi n[Ae^{-\lambda_g t}+Be^{-\lambda_m t}]. \quad (2)$$

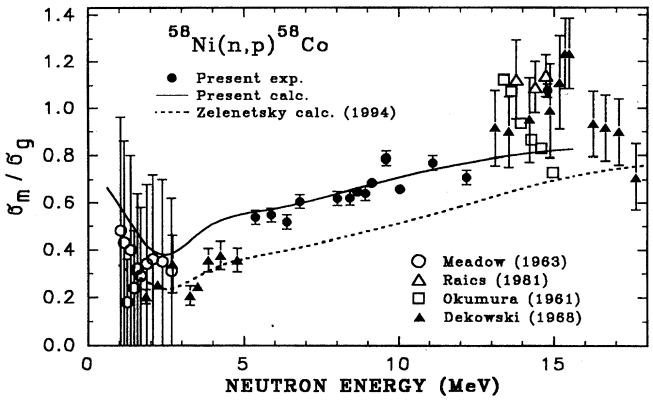

FIG. 4. Isomeric cross section ratio for the production of $^{58}Co^{m,g}$ as a function of incident neutron energy.

Details of the determination of the σ^m/σ^g ratio from Eq. (2) can be found in (cf. Ref. [37]). The experimental results of the isomeric cross section ratio vs neutron energy are given in Table III. Over the energy range between 5–13 MeV all the data reported here have been measured for the first time. The measured total ($\sigma^m+\sigma^g$) and isomeric (σ^m) cross section as well as the isomeric ratio (σ^m/σ^g) versus neutron energy rendered possible to deduce some additional data both for σ^m/σ^g and σ^m values as indicated in Tables III and IV. In Fig. 4 our experimental and calculated σ^m/σ^g values together with the literature data (cf. Refs. [5,6,38,39]) are presented. As shown in Fig. 4 our model calculation can reproduce the shape and magnitude of the isomeric cross section ratio fairly well indicating the possible use of the adopted model parameters. At energies around 14 MeV the two independent calculations give lower σ^m/σ^g ratios than the experiments. It should be noted, however, that the measured data at around 14 MeV are discrepant. The error bars in the 1–3 MeV range prevent to observe any structure in the $\sigma^m/\sigma^g(E)$ function, however, the calculations follow the trend of the measured data and exhibit a minimum at around 2.5 MeV. Further measurements with high precision are required to prove the existence of this minimum.

Zelenetsky's calculation for the $\sigma^m/\sigma^g(E)$ function is systematically lower than the experimental data in the 5–14 MeV range. The deviations between these two results may arise from the differences in the number of discrete levels, branching ratios and level density models accepted for the calculations. The measured and calculated $\sigma^m/\sigma^g(E)$ functions show a definite increase with the projectile energy from 2.5 to 15 MeV which indicates that the high spin (5^+) isomeric state is preferentially populated at higher energies.

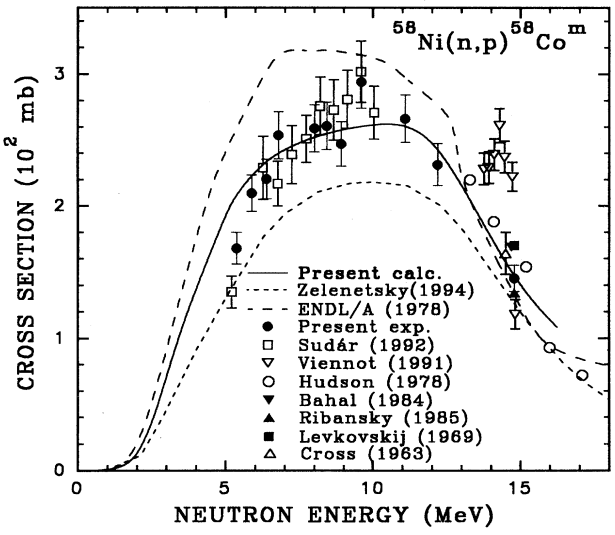

FIG. 5. Measured, calculated, and evaluated excitation functions for the $^{58}Ni(n,p)^{58}Co^m$ reaction.

The measured total activation cross sections and isomeric cross section ratios rendered possible to determine the excitation function of the $^{58}Ni(n,p)^{58}Co^m$ reaction. Results deduced from these two data sets are presented in Table IV. These data agrees well with those obtained in an our previous measurement (cf. Ref. [40]) based on the detection of Co x rays for the determination of σ^m values in the 5–10 MeV range. In Fig. 5 the measured, calculated, and evaluated data are summarized for the $\sigma^m(E)$ function. As can be seen in the figure our calculation agrees well with the available experimental data (cf. Refs. [41–47]) but deviates significantly from both the ENDL/A evaluation (cf. Ref. [16]), and Zelenetsky's calculation. The shapes of the $\sigma^g(E)$ and $\sigma^m(E)$ functions beyond 12 MeV prove the increasing trend in the σ^m/σ^g ratio with the bombarding neutron energy. Further measurements are in progress to increase the accuracy of the data for the σ^m/σ^g ratio from the threshold to 15 MeV.

ACKNOWLEDGMENTS

The authors are grateful to Professor H. Vonach for the valuable discussion. Thanks are due to Mr. J. Szegedi for the technical assistance during the irradiations. This work was supported by the Hungarian Research Foundation Contract No. 1734/91, T016713/95, and the International Atomic Energy Agency Contract No. 7687/RB.

[1] A. Pavlik, G. Winkler, and M. Uhl, Nucl. Sci. Eng. **90**, 186 (1985).

[2] J. F. Barry, J. Nucl. Energy **16**, 467 (1962).

[3] D. L. Smith, J. W. Meadows, H. Vonach, M. Wagner, R. C. Haight, and W. Mannhart, in *Proceedings of the International Conference on Nuclear Data for Science and Technology*, Jülich, 1991, edited by S. M. Qaim (Springer-Verlag, Berlin, 1991), p. 282.

[4] D. L. Smith and J. W. Meadows, ANL Report No. ANL-7989, 1973; D. L. Smith and J. W. Meadows, ANL Report No. ANL/NDM-10, 1975.

[5] J. W. Meadows and J. F. Whalen, Phys. Rev. **130**, 2022 (1963).

[6] P. Raics, F. Pászti, S. Daróczy, and S. Nagy, ATOMKI Kozl. **23**, 45 (1981).
[7] Fan Peiguo, Zhao Wenrong, Teng Dan, and Lu Hanlin, Chinese J. Nucl. Phys. **7**, 242 (1985).
[8] N. V. Kornilov, V. Baryba, A. V. Balickij, A. C. Rudenko, S. Daróczy, P. Raics, and S. Nagy, At. Energ. **58**, 128 (1985).
[9] Zhao Wenrong, Lu Hanlin, You Weixiang, and Yuan Xialin, "Compilation of Measurements and Evaluations of Nuclear Activation Cross Sections for Nuclear Data Applications," IAEA, INDC (CPR-16), 1989.
[10] H. D. Lemmel, IAEA, Report No. IAEA-NDS-100, Rev. 3, The United States Evaluated Nuclear Data Files (B-VI), 1990.
[11] A. V. Zelenetsky (private communication).
[12] V. Avrigeanu, P. E. Hodgson, and M. Avrigeanu, Phys. Rev. C **49**, 2136 (1994).
[13] Computer Index of Nuclear Data-94 (1988–1994), The Index to Literature and Computer Files on Microscopic Neutron Data," IAEA Report, Vienna, 1994.
[14] V. McLane, C. L. Dunford, and P. Rose, *Neutron Cross Sections* (Academic, New York, 1988), Vol. 2.
[15] J. Kopecky, Report No. EAF-Doc-6, Netherlands Energy Research Foundation, Petten, 1994.
[16] Activation File of the Evaluated Nuclear Data Library of 1982, Report No. UCRL-50400, Vol. 18, 1978, Lawrence Livermore National Laboratory, 1978.
[17] J. Csikai, *Handbook of Fast Neutron Generators* (CRC Press, Boca Raton, 1987), Vols. I and II.
[18] A. Grallert, J. Csikai, and S. M. Qaim, Nucl. Instrum. Methods Phys. Res. Sect. A **337**, 615 (1994).
[19] F. E. Chukreev, "Selection of Radiaton Sources for Calibration of Gamma-Ray Spectrometers," Report No. INDC(CCP)-361, IAEA, 1994.
[20] "X-ray and gamma-ray standards for detector calibration," Report No. IAEA-TECDOC-619, IAEA, 1991.
[21] W. Mannhart and H. Vonach, Nucl. Instrum. Methods **136**, 109 (1976).
[22] A. Pavlik and G. Winkler, Report No. INDC(AUS)-011/LI, IAEA, 1986.
[23] *Table of Isotopes*, 7th ed., edited by C. M. Lederer and V. S. Shirley (Wiley, New York, 1978).
[24] S. Cabral, B. Börker, H. Klein, and W. Mannhart, Nucl. Sci. Eng. **106**, 308 (1990).
[25] A. Grallert, J. Csikai, S. M. Qaim, and J. Kniepers, Nucl. Instrum. Methods Phys. Res. Sect. A **334**, 154 (1993).
[26] J. Csikai, A. Grallert, L. Oláh, and S. M. Qaim, in *Proceedings of the International Conference on Nuclear Data for Science and Technology*, Gatlinburg, Tennesse, 1994, edited by J. K. Dickens (American Nuclear Society), LaGrange Park, IL, 1994), p. 78.
[27] W. Mannhart, in *Handbook on Nuclear Activation Data*, IAEA Technical Report Series No. 273 (IAEA Vienna, 1987), pp. 163 and 413.
[28] M. Uhl and B. Strohmaier, IRK Report No. 76/01, 1976.
[29] O. Bersillon, Report No. CEA-N, 2227, 1981.
[30] F. D. Becchetti and G. W. Greenlees, Phys. Rev. **182**, 1190 (1969).
[31] F. G. Perey, Phys. Rev. **131**, 745 (1962).
[32] L. McFadden and G. R. Satchler, Nucl. Phys. **84**, 177 (1966).
[33] M. Uhl, H. Gruppelaar, H. A. J. van der Kamp, J. Kopecky, and D. Nierop in [3], p. 924.
[34] A. H. Wapstra and K. Bos, At. Data Nucl. Data Tables **19**, 215 (1977).
[35] T. W. Burrows and M. R. Bhat, Nucl. Data Sheets **47**, 1 (1986); L. K. Peker, *ibid.* **42**, 457 (1984); Z. Enchen, H. Junde, Z. Chunmei, L. Xiane, and W. Lizheng, *ibid.* **44**, 463 (1985); H. Verhuel and R. L. Auble, *ibid.* **23**, 455 (1978); R. L. Auble, *ibid.* **20**, 253 (1977); P. Anderson, L. P. Ekström, and J. Lyttkens, *ibid.* **39**, 641 (1983).
[36] W. Dilg, W. Schantl, H. Vonach, and M. Uhl, Nucl. Phys. **A217**, 269 (1973).
[37] F. Cserpák, S. Sudár, J. Csikai, and S. M. Qaim, Phys. Rev. C **49**, 1525 (1994).
[38] P. Decowski, W. Grochulski, A. Marcinkowski, K. Siwek, I. Sledzinska, and Z. Wilhelmi, Nucl. Phys. **A112**, 513 (1968).
[39] Shoji Okumura, Nucl. Phys. **A93**, 74 (1967).
[40] S. Sudár, J. Csikai, S. M. Qaim, and G. Stöcklin in [3], p. 291.
[41] M. Viennot, A. Ait Haddou, A. Chiadli, and G. Paic, University of Mohammed V., Rabat, Morocco, Report No. P.MOH-5, **10**, 1982.
[42] M. Viennot, M. Berrada, G. Paic, and S. Joly, J. Nucl. Sci. Eng. **108**, 289 (1991).
[43] C. G. Hudson, W. L. Alford, and S. K. Ghorai, J. Ann. Nucl. Energy **5**, 589 (1978).
[44] B. M. Bahal and R. Pepelnik, Report No. GKSS-84-E, GKSS (Gesellschaft für Kernenergie-Verwertung in Schiffbau und Schiffahrt)-Forshungszentrum Geesthacht GmbH, Geesthacht, 1984.
[45] I. Ribansky, J. Kristiak, L. Stoeva, and C. Panteleev, Report No. INDC(CSR)-7, IAEA, Vienna, 1985.
[46] V. N. Levkovskij, G. P. Vinitskaja, G. E. Kovel'skaja, and V. M. Stepanov, Yad. Fiz., **10** (1), 44 (1969).
[47] W. G. Cross, R. L. Clarce, K. Morin, G. Slinn, N. M. Ahmed, and K. Beg, Report No. EANDC(CAN)-16, 1963, European-American Nuclear Data Committee Documents, p. 1.